JSEE Vol. 21, No. 4, 2019 DOI:10.48303/jsee.2019.243310

Initial Solution for Designing a Soft Substructure in a Mass Isolation System with Consideration of Stability Constraints

Mohammad Boujary[1] and Mansour Ziyaeifar[2*]

1. Ph.D. Candidate, International Institute of Earthquake Engineering and Seismology (IIEES), Tehran, Iran
2. Associate Professor, Structural Engineering Research Center, International Institute of Earthquake Engineering and Seismology (IIEES), Tehran, Iran,
*Corresponding Author; email: Mansour@iiees.ac.ir

Received: 11/05/2020
Accepted: 18/10/2020

ABSTRACT

The new techniques in seismic design of structures are usually attributed to high damping ratios. Mass isolation of structures is one of the new techniques in seismic design of structures that focuses on the mass of the structure as the main target for seismic isolation and reducing earthquake effects on buildings. Mass Isolation System (MIS) consists of two stiff and soft substructures connected by a viscous damper. The mass subsystem comprises the main mass of the structure, which is attached to a frame with a low stiffness by a separation mechanism at the height of the structure including viscous dampers to a stiffness subsystem consisting of a moment or braced frame system with great stiffness. In this paper, the aim is to present a simple preliminary design method based on the normalized pushover curve. The most important problems for increasing the period of the soft structure are deformation and structural stability. This paper presents a preliminary design solution for a soft substructure of the Mass Isolation System (MIS) with consideration of stability constraints. To this end, the paper presents mathematical relationships to calculate the period of the structure followed by proposing a simple solution for the design of the soft substructure.

Keywords:
Mass Isolation System; Stability; Period; P-Δ effect; Collapse Prevention

1. Introduction

Modern methods of seismic performance control, commonly known as performance control techniques, often seek to dissipate seismic energy by increasing the flexibility of the structure. One of these techniques is the connection of two adjacent structures by dampers [1-2]. This method can also be used for a single structure by separating the gravity load system from the lateral load system [3-4]. It has been shown that increasing the period difference between these two substructures will improve the performance of this method. The proposed system is known as the Mass Isolation System (MIS). Such structures can be modeled according to Figure (1).

The MIS can be divided into two substructures, the mass substructure in which most of the mass of the structure is concentrated and the stiff substructure from which most of the lateral stiffness of the structure is derived (Figure 2). The two substructures are connected by a viscous damper to reduce the displacement amplitude of the mass substructure, and the stiff substructure acts as a support for the dampers, which act as an energy dissipation system [3-4]. Due to the low lateral stiffness of the soft substructure, theoretically and

according to the seismic design spectrum, the best design for the soft substructure is to increase its period as much as possible to reduce the seismic base shear. Therefore, it can be assumed that this structure is designed exclusively for gravity forces and without the effects of lateral forces. However, excessive increase of structural period, and consequently excessive reduction of lateral stiffness can lead to structural instability. On the other hand, the hard infrastructure, as the lateral support of the dampers, must have a high lateral stiffness to withstand the forces transferred from the dampers. Of course, it may be a mistake to say that due to the high stiffness of the stiff substructure, the seismic shear base of this structure would be large and irrational. However, it should be noted that despite the high stiffness of this structure, its seismic base shear will not be high, because this structure will have a small mass compared to its considerable stiffness.

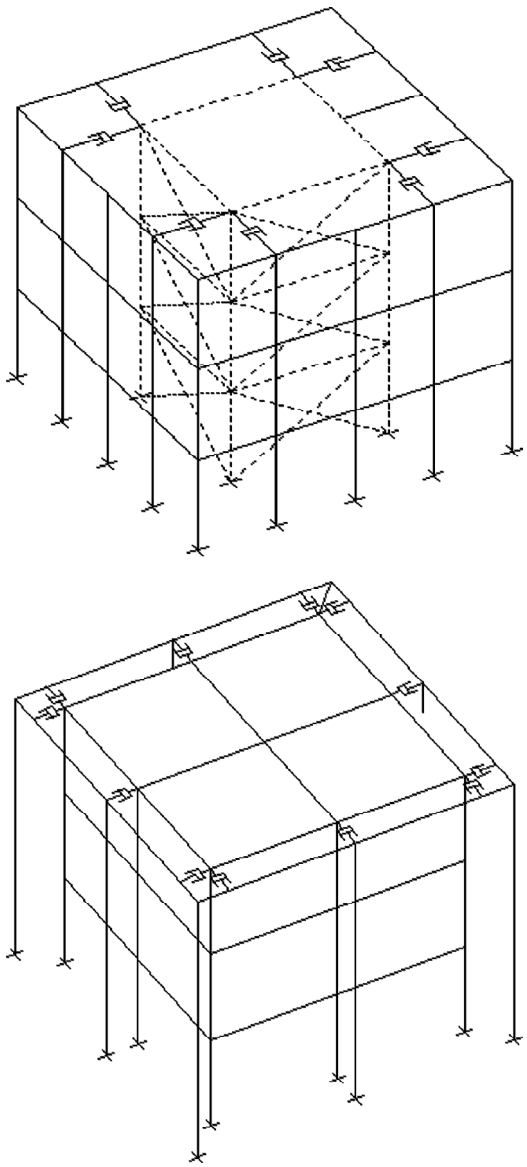

Figure 1. Simplified model of the mass isolation system.

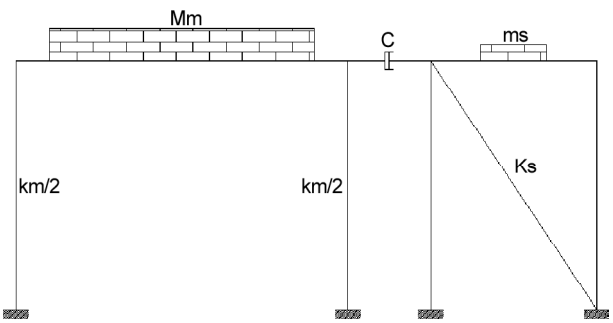

Figure 2. Two-mass modeling.

The design criterion for a soft structure should be based on the displacement control method, since the major part of the seismic forces in this part of the structure is transmitted through a damper to a stiff structure. It can be shown that there is always a reciprocal relationship between the period and the stability ratio, and this relation can be expressed as $T = \alpha\lambda^{-\beta}$. The coefficients α and β are determined with respect to the height of the structure and other structural parameters, and λ from eigen-analysis of structural stiffness matrix is determined by taking into account the effects of P-Δ and the concept of the gravity increase factor of the structure to achieve instability due to the structural weight. Therefore, the aim of this paper is to implement the design of high-damping structures (and in particular, Mass Isolation Systems), considering the proper and safe stability limits, the minimum stability ratio for the frame structures is determined and, finally, the period of the soft structure Calculated. The method of doing work is based on a combination of nonlinear push-over and dynamic methods, taking into account the gravity load effects.

2. Procedures for Calculation of Stability Factor

Sideways collapse of the structure subjected to severe earthquake excitation is due to the successive reduction of lateral load capacity as a result of the stiffness and strength deterioration, and the global destabilizing effect of gravity loads acting through lateral displacements (P-Delta effect) [5]. In very flexible buildings, the destabilizing effect of gravity loads may lead to a negative post-yield stiffness, and as a consequence, the structural collapse capacity might be exhausted at a rapid rate

when the earthquake drives the structure into its inelastic range of deformation, even for stable hysteretic component behavior [6]. The excessive deformation of the mass structure may have undesirable effects on the stability of the structure. Even this parameter has not been directly investigated in nonlinear push-over analysis and nonlinear time histories, and only the general buckling of the members is considered in nonlinear calculations. Therefore, the criterion for determining the performance of IO, LS, or CP is merely the formation of hinges in structural elements, and the general stability of the structure is ignored in this regard, while according to studies, the change in the axial load pattern in the members as well as the formation of plastic joints can affect the structural stability.

In Figure (3), the behavior of a structure is seen with and without regard to the secondary moments of the effect caused by P-Δ. As it is seen, taking into account the decreasing effects of the geometric hardness matrix and the secondary moments reduces the initial stiffness of the pushover structure as well as the expected resistance of the structure. In addition, the behavior of the structure after reaching the yield limit with negative and decreasing stiffness goes down. In this section, how to calculate the amount of these impacts and their effects will be examined.

However, none of the codes explicitly provides documentary evidence of the reliability ratio versus stability for the entire structure, and only refers to the ASCE 7-10 code to calculate the limit of instability (known as the maximum stability index), which is the safety factor of 2 [7].

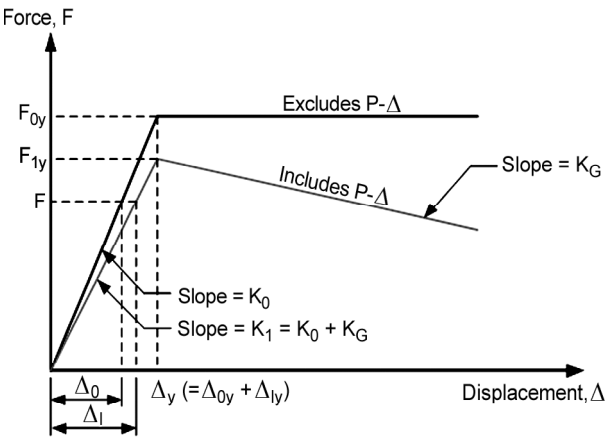

Figure 3. An ideal response of a 1-Story structure, with and without P-Δ effect [7].

The collapse capacity of inelastic P-Delta sensitive frames has been investigated in numerous articles [8-11]. According to a study by Bernal [12] focused on two-dimensional frames and aimed at determining the minimum lateral stiffness needed for the frame, he presented the coefficient of stability with the dynamic modeling of the structure and assuming non-linear behavior for the frame.

$$\theta_i = \frac{k_{gi}}{\omega_\circ^2 m_i} \tag{1}$$

where θ_i is the coefficient of stability of the frame after the formation of ith plastic mode. Also, Bernal [13] showed that the stability index can be expressed by its dependence on the mode forms.

$$\theta = \frac{\{\phi_1\}^T \left[K_g\right]\{\phi_1\}}{\{\phi_1\}^T \left[K_\circ\right]\{\phi_1\}} = \frac{K_{g_1}}{K_1} \tag{2}$$

where $\{\phi_1\}$ is the shape of the first mode, K_g is the geometric stiffness matrix, and $K_\circ$ is the linear structure stiffness matrix, K_{g_1} and K_1 are the geometric stiffness matrix and the stiffness matrix of the first mode of the structure, respectively.

Accordingly, and in continuation of their work, the empirical equations for calculating the stability index of the linear state $\theta_\circ$ and the stability index equal to the failure of the frame θ_m are as follows [9, 12]:

$$\theta_\circ = \frac{3Ng\tau}{(2N+1)\omega_\circ^2 h}$$
$$\theta_m = \frac{\Omega g \tau}{\omega_\circ^2 h} \tag{3}$$

where N is the number of stories, g is the gravity acceleration, h is the total building height, τ is the ratio of total weight to effective seismic weight.

$$\tau = \frac{P_u}{W} = \frac{D + 0.5L}{D + 0.2L} \tag{4}$$

The critical mechanism for analyzing dynamic stability can be roughly the same as the static failure mechanism due to a pushover analysis with lateral load distributions relative to mass [13]. It has also been shown that the failure mechanism in buildings is statistically independent of the fact that the excitation is near the fault or far from the fault [9].

The mentioned analyzes are an introduction to the application of the stability index in seismic codes.

As an example, according to the ASCE 7-10 code [14], the structural stability is achieved by the following equation:

$$\theta = \left| \frac{P\Delta_\circ}{F_\circ h_{sx}} \right| \tag{5}$$

where h_{sx} is the story height, $F_\circ$ is the shear force in story such as $\Delta_\circ, \Delta_\circ$ is the elastic lateral story drift, which is equal to $\Delta I_e / C_d$, Δ is the inelastic story drift determined in accordance with Section 12.8.6 in ASCE 7-10 Standard, and P is the total gravity load supported by the structure.

By comparing this coefficient of stability index based on Equation (2) with the stability factor of the frames mentioned in [15], it can be concluded that:

$$\lambda_1 = \frac{K_1}{K_{g1}} = \frac{1}{\theta} \tag{6}$$

where λ_1 is the coefficient of frame stability in the first mode.

Based on Bernal studies, the nonlinear behavior curve of a structure under the effect of increasing load (pushover curve) can be summarized in the bilinear form below:

The additional parameters used in this figure are defined as follows:

$$\begin{aligned} \bar{\theta} &= \frac{\theta_m}{Q} \\ \bar{\omega}_\circ^2 &= \omega_\circ^2 Q \\ \bar{S}_{au} &= S_{au} Q \\ Q &= 1 - \theta_\circ + \theta_m \end{aligned} \tag{7}$$

Yield displacement is almost independent of the nonlinear geometric effects of P-Δ [15]. It has also been shown in studies that the initial period (and therefore the initial stiffness) does not play an important role in determining the boundary of instability [13]. As a result, immunity against dynamic instabilities is not guaranteed by controlling the initial elastic stiffness, and a reasonable method of checking safety against this failure mode should be considered by examining the strength and shape of the mechanism of the critical mechanism [13].

Theoretically, a system may persist after a transient response to a dynamic stimulation or even exceed the static stability ($\lambda_s = 1/\theta_\circ$), but numerical results show that, for an earthquake stimulation, with a considerable time, the threshold of dynamic instability (λ_d) is much less than λ_s [16]. For example, Castilla and Lopez [17] have suggested that λ_d be considered to be $\lambda_s^{0.5}$.

By defining the ratio between the maximum factored gravity load, P_u and the gravity load assumed present during the earthquake, P_s:

$$\beta = \frac{P_u}{P_s} \tag{8}$$

The ductility should be limited to μ_m given by [16]:

$$\mu_m = \frac{1}{\beta\theta} = \frac{\lambda_s}{\beta} \tag{9}$$

Assuming a capacity reduction factor ϕ β can be expressed as follows:

$$\beta = \frac{(1.2D + 1.6L)}{\phi(D + 0.2L)} \tag{10}$$

Assuming $L/D = 0.4$ (which is reasonable for buildings) and $\phi = 0.75$:

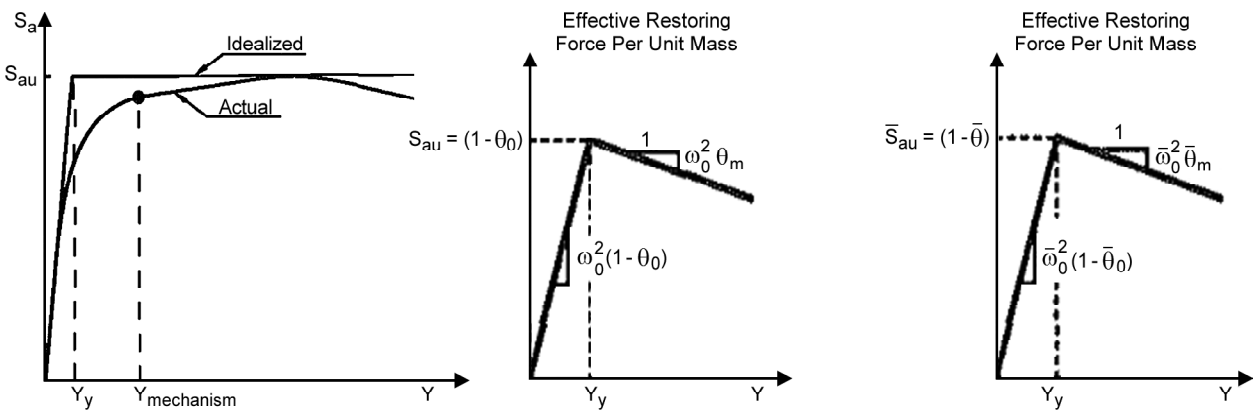

Figure 4. Effective restoring force per unit mass versus generalized displacement [12].

$$\beta = 2.25 \Rightarrow \mu_m = \frac{0.45}{\theta} = 0.45\lambda_s \quad (11)$$

Considering Figure (5), there are three ideal curves for non-linear pushover behavior. The top curve represents a case of no gravity, the intermediate curve is for the axial load present during the design earthquake (proportional to the effective seismic load), and the lower one corresponds to the factored gravity loads [16].

The maximum permanent deformation, considering the ductility μ, is:

$$\Delta_f = \mu\Delta_y - \Delta_\circ \quad (12)$$

where:

$$\Delta_\circ = \frac{B}{K_\circ(1-\theta)}$$
$$B = R_{y_\circ}(1-\theta) - C \quad (13)$$
$$C = \theta K_\circ \Delta_y(\mu - 1)$$

Substituting the second and third equations into the first equation, and recognizing that $R_{y_\circ} = K_\circ\Delta_y$ one gets:

$$\Delta_\circ = \Delta_y \frac{(1-\mu\theta)}{(1-\theta)} \quad (14)$$

And as a result:

$$\Delta_f = \Delta_y \frac{(\mu-1)}{(1-\theta)} \quad (15)$$

Due to the permanent deformation, Δ_f, increasing gravity load increases the lateral drift. This effect is indicated by arrows in the figure. The general expression for the additional drift is:

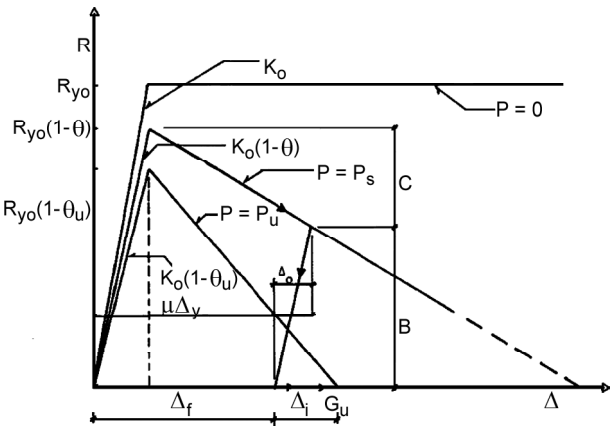

Figure 5. The ideal curve of structural pushover behavior [16].

$$\Delta_i = (P_u - P_s)\frac{\Delta_f}{K_\circ H(1-\theta_u)}$$
$$\theta_u = \frac{P_u}{K_\circ H} \quad (16)$$

From the figure:

$$G_u = \Delta_f + \Delta_i \quad (17)$$

Substituting equations:

$$G_u = \Delta_y \frac{(\mu-1)}{(1-\theta)}\left(1 + \frac{(P_u - P_s)}{K_\circ H(1-\theta_u)}\right) \quad (18)$$

$$G_u = \Delta_y \frac{(\mu-1)}{(1-\theta)}\left(1 + \frac{(P_u - P_s)}{K_\circ H(1-\theta_u)}\right)$$

With β from Equation (10) and noting that $\theta_u = \beta\theta$ Equation (20) can be expressed as:

$$G_u = \Delta_y \frac{(\mu-1)}{(1-\beta\theta)} \quad (19)$$

G_u is also given by:

$$G_u = \frac{\Delta_y}{\theta_u} = \frac{\Delta_y}{\beta\theta} \quad (20)$$

However, in spite of all the issues raised, due to the considerable reduction in the soft structure displacement due to the connection to the hard structure and the use of high damping ratios, the problem of stability should be examined from a different viewpoint in order to allow the softness of the soft structure to be increased. As a result, the period will be set to higher values than usual.

3. Presentation of a Design Method based on Stability with Limited and Controlled Displacement

In this section, by assuming the stability parameter as a design parameter, and not just a check parameter at the end of the design process, in accordance with the desired application of the soft structure, for this structure, the minimum amount of safe stability factor is determined, and as a result, the seismic base shear is recommended.

First, the minimum stability factor of the frame must be determined so that, with the assumption of 0.5 to 0.7 percent of the drift for this particular structure, the structural stability is maintained.

According to ASCE 7-10, in most structures, if the stability index value exceeds 0.25, the structure has an unstable risk and should be redesigned. This amount of the stability index, is equivalent to reducing stability factor of 4, the structure will be at the risk of instability and, accordingly, the stability factor of less than 4 for the structure will be unacceptable, and according to the point earlier, ASCE 7-10 was said to have included a safety factor of 2 in calculating this value.

Also, according to the above-mentioned equations, the following equations can be reached to estimate the minimum stability factor:

$$\left.\begin{aligned}\Delta_{r,\max} &= \left(C_d - \frac{1}{\beta}\right)\Delta_\circ \\ \Delta_r &= \Delta_y \frac{(\mu-1)}{(1-\theta)}\end{aligned}\right\} \xrightarrow[\text{usually } \beta=1]{\Delta_r=\Delta_{r,\max}}$$

$$C_d - 1 = \frac{(\mu-1)}{(1-\theta)} \xrightarrow[\mu=\frac{1}{\beta_u\theta}=\frac{\lambda_s}{\beta_u}]{\theta=1/\lambda_s}$$

$$C_d = \frac{\lambda_s(\lambda_s-\beta_u)}{\beta_u(\lambda_s-1)} + 1 \Rightarrow \tag{21}$$

$$\lambda_s^2 - \beta_u C_d \lambda_s + \beta_u (C_d - 1) = 0$$

$$\beta_u = \frac{(1.2D + 1.6L)}{\phi(D + 0.2L)}$$

$$\theta_{\max} = \frac{0.5}{\beta C_d - 1} \xrightarrow{\text{usually } \beta=1} \theta_{\max} = \frac{0.5}{C_d - 1} \Rightarrow$$

$$\lambda_{\min} = \frac{C_d - 1}{0.5} = 2(C_d - 1) \tag{22}$$

It should be noted that for reliability, ASCE allows $\beta = 1.0$ to be assumed [18]. Regarding Equations (21) and (22), having the coefficient C_d, the lowest acceptable stability factor can be obtained by assuming a safety coefficient 2 to maintain the stability and expected value for the stability factor.

For example, ASCE [18] proposes the deflection amplification factor of 5.5 for steel special moment frames. As a result, according to Equations (21) and (22), the minimum safe coefficient for such structures will be equal to:

$$C_d = 5.5$$

$$\text{Guess}: \quad \phi_b = 0.9 \quad \& \quad L/D = 0.4$$

$$\beta_u = \frac{(1.2D + 1.6L)}{\phi(D + 0.2L)} = \frac{1.2 + 1.6 \times 0.4}{0.9(1 + 0.2 \times 0.4)} = 1.893$$

$$\lambda_s^2 - \beta_u C_d \lambda_s + \beta_u (C_d - 1) = 0 \rightarrow$$

$$\lambda_s^2 - 10.412\lambda_s + 8.519 = 0 \Rightarrow$$

$$\lambda_s = \begin{cases} 9.52 \\ 0.90 \end{cases} \geq \lambda_{\min} = 2(C_d - 1) = 9 \Rightarrow \lambda_s = 9.5$$

This means that in order to maintain the stability of the structure to withstand the ultimate displacement proposed by ASCE, the stability factor of the structure must be at least 9.5 or in other words, the stability index in all stories must not exceed 0.11.

Similarly for steel ordinary moment frames, the following result will be obtained:

$$C_d = 3$$

$$\lambda_s^2 - 5.679\lambda_s + 3.786 = 0 \Rightarrow$$

$$\lambda_s = \begin{cases} 4.91 \\ 0.77 \end{cases} \geq \lambda_{\min} = 4 \Rightarrow \lambda_s = 4.91$$

With the logical assumption and with the use of the Bernal presentation equations, the following method is proposed for soft structure design. In this method, the stability factor is calculated first by assuming the minimum coefficient of stability for the structure (for example, 5, 25% higher than the minimum accepted by ASCE). Then, the probable period of the structure is estimated using the following relationship.

$$T = 2\pi\sqrt{\frac{(2N+1)h}{3Ng\tau\lambda}} \tag{23}$$

As previously stated, assuming $L/D = 0.4$, the value of the coefficient τ is equal to 1.11. By assuming the same stories height of 3.3 m for the structure, the above relation can be simplified as follows.

$$\left.\begin{aligned} h &= 3.3N \\ \tau &= 1.11 \end{aligned}\right\} \Rightarrow T = 2\pi\sqrt{\frac{(2N+1)}{g\lambda}} \tag{24}$$

Then, in accordance with the standard criteria and using the equivalent static method, the design base shear for this structure is calculated to obtain the minimum lateral stiffness to ensure the stability of the structure.

As a result, the following two methods are proposed for the design of structures with a limited and controlled displacement and with a stability limitation.

In the first method, due to the collapse acceleration proposed by Bernal [12] and its ratio with the ultimate acceleration, $I_c = 1.7$, and the collapse acceleration in the structure is assumed to be in the design limit, y_u. Therefore, assuming the value of the stability factor $\lambda = 5$ and design drift y_u, for short structures 1.5% and for mid-rise structures 2.0%, and the coefficient $I_c = 1.7$ the ultimate acceleration value for the structure S_{au} is calculated, and assuming the overstrain coefficient $\Omega = 2$, the acceleration of the design limit S_d is calculated and the structure is designed to withstand this base acceleration.

In the second method, the assumption is used that the yielding displacement is approximately independent of the nonlinear geometric P-Δ effects [15]; the same as in the first method, but by considering y_y to be equal to the proposed values in FEMA 273 [19] for Immediate Occupancy level (IO), and selecting the stability factor λ for each structure so that $y_f = \Delta_f / H$ is more than 1.0% (Δ_f as shown in Figure 5) and preserved $I_c = 1.7$. Accordingly, as in the first method, calculating S_{au} and assuming the overstrain coefficient $\Omega = 2$, the acceleration of the design limit S_d is calculated and the structure is designed to withstand this base acceleration.

To examine the proposed methods, the following equations are extracted according to Figure (4). If the equations of the ascending and descending branches of the curve are denoted by S_1 and S_2, respectively, then:

$$S_1 = \bar{\omega}_\circ^{\,2}\left(1-\bar{\theta}\right)Y$$

$$S_2 = \bar{S}_{au}\left(1-\bar{\theta}\right) - \bar{\omega}_\circ^{\,2}\bar{\theta}\left(Y - Y_y\right) = -\bar{\omega}_\circ^{\,2}\bar{\theta}\left(Y - Y_u\right)$$

All of the above parameters are defined in Figure (4), and Y_u is the final displacement of the curve (i.e., the point where the value of S equals zero (see Figure 5)). As a result, it can be easily shown that:

$$\bar{S}_{au} = \bar{\omega}_\circ^{\,2} Y_y \tag{25}$$

It can also be shown that:

$$S_2\left(Y_y\right) = \bar{S}_{au}\left(1-\bar{\theta}\right) \rightarrow \bar{S}_{au}\left(1-\bar{\theta}\right) =$$

$$-\bar{\omega}_\circ^{\,2}\bar{\theta}\left(Y_y - Y_u\right) \xrightarrow{\bar{S}_{au} = \bar{\omega}_\circ^{\,2} Y_y} \rightarrow$$

$$\bar{\omega}_\circ^{\,2} Y_y\left(1-\bar{\theta}\right) = \bar{\omega}_\circ^{\,2}\bar{\theta}\left(Y_u - Y_y\right)$$

As a result, it can be concluded that:

$$Y_y = \bar{\theta} Y_u \tag{26}$$

Also according to Bernal [12] ($(S_{ac} = S_{au} / I_c)$ if a displacement such as S_{ac} is indicated by Y_d :

$$S_2\left(Y_d\right) = \bar{S}_{ac}\left(1-\bar{\theta}\right) = \frac{\bar{S}_{au}}{I_c}\left(1-\bar{\theta}\right) \rightarrow$$

$$\frac{\bar{S}_{au}}{I_c}\left(1-\bar{\theta}\right) = -\bar{\omega}_\circ^{\,2}\bar{\theta}\left(Y_d - Y_u\right) \xrightarrow{\bar{S}_{au} = \bar{\omega}_\circ^{\,2} Y_y} \rightarrow$$

$$\frac{\bar{\omega}_\circ^{\,2} Y_y}{I_c}\left(1-\bar{\theta}\right) = \bar{\omega}_\circ^{\,2}\bar{\theta}\left(Y_u - Y_y\right) \xrightarrow{Y_y = \bar{\theta} Y_u} \rightarrow$$

$$\frac{\bar{\omega}_\circ^{\,2}\bar{\theta} Y_u}{I_c}\left(1-\bar{\theta}\right) = \bar{\omega}_\circ^{\,2}\bar{\theta}\left(Y_u - Y_y\right)$$

It can be concluded that:

$$Y_d = Y_u\left(1 - \frac{1}{I_c}\left(1-\bar{\theta}\right)\right) \tag{27}$$

If the seismic response coefficient is defined as $C = \bar{S}_{ac}\left(1-\bar{\theta}\right)/g$, for example, for a 4-story structure with the story height of 3.3 m, the two proposed methods will be considered as follows:

Method 1:

$N = 4, \quad \mathrm{h} = 3.3\,\mathrm{m}, \quad L/D = 0.4,$

$g = 9.806\frac{m}{s^2}, \quad \lambda = 6, \quad \delta_u = 1.5\%, \quad I_c = 1.7$

$$\theta_\circ = \theta_m = \theta = \frac{1}{\lambda} = 0.167 \rightarrow$$

$$Q = 1 - \theta_\circ - \theta_m = 1 \rightarrow \bar{\theta} = 0.167$$

$$\tau = \frac{D + 0.5L}{D + 0.2L} = 1.11 \rightarrow$$

$$T = 2\pi\sqrt{\frac{(2N+1)H}{3Ng\tau\lambda}} = 2.45\,s \rightarrow \bar{\omega} = \frac{2\pi}{T}Q = 2.57\frac{rad}{s}$$

$$Y_u = \delta_u H = 19.8\,cm \rightarrow Y_y = Y_u\bar{\theta} = 3.3\,cm$$

$$S_{au} = Y_y\bar{\omega}^2 = 0.218\frac{m}{s^2} \rightarrow S_{ac} = \frac{S_{au}}{I_c} = 0.128\frac{m}{s^2} \Rightarrow$$

$$C = \frac{S_{ac}}{g}\left(1-\bar{\theta}\right) = 0.011$$

Method 2:

$N = 4, \quad \mathrm{h} = 3.3\,\mathrm{m}, \quad L/D = 0.4,$

$g = 9.806\frac{m}{s^2}, \quad \lambda = 6, \quad \delta_d = 1.5\%, \quad I_c = 1.7$

$$\theta_\circ = \theta_m = \theta = \frac{1}{\lambda} = 0.167 \rightarrow$$

$$Q = 1 - \theta_\circ - \theta_m = 1 \rightarrow \bar{\theta} = 0.167$$

$$\tau = \frac{D+0.5L}{D+0.2L} = 1.11 \rightarrow T = 2\pi\sqrt{\frac{(2N+1)H}{3Ng\tau\lambda}} = 2.45s \rightarrow$$

$$\bar{\omega} = \frac{2\pi}{T}Q = 2.57\frac{rad}{s}$$

$$\delta_u = \frac{\delta_d}{1-\frac{1}{I_c}(1-\bar{\theta})} = 2.94\% \rightarrow Y_u = \delta_u H = 38.8cm \rightarrow$$

$$Y_y = Y_u\bar{\theta} = 6.5cm$$

$$S_{au} = Y_y\bar{\omega}^2 = 0.427\frac{m}{s^2} \rightarrow S_{ac} = \frac{S_{au}}{I_c} = 0.251\frac{m}{s^2} \Rightarrow$$

$$C = \frac{S_{ac}}{g}(1-\bar{\theta}) = 0.021$$

4. Numerical Modeling

To investigate the proposed methods, three two-dimensional frames were selected, which are shown in Figure (6). First, each frame is modeled and designed according to standard criteria. Then, according to the two methods proposed in the previous section, period and seismic response coefficient of structures using the techniques that will be discussed later, the structures are redesigned to achieve the period calculated according to Equation (24). Then, for each structure, the pushover analysis will be performed and a bilinear curve will be generated for them. Finally, to ensure the stability of the structure, the stability factor of the structure before and after push is calculated and compared with the minimum acceptable value (λ = 4.0 discussed in previous sections).

First, these three structures were designed according to Iranian 2800 code and their basic parameters were extracted, as shown in Table (1).

1. General Collapse Behavior: In this method, according to the relations provided by Bernal [12] and assuming the general mechanism ($G/h = 1.0$), the final acceleration and critical gravity acceleration are calculated and the structure for critical base shear (V_c) has been redesigned.
2. Maximum period using standard relationship: In this method, assuming a minimum of 6 for the stability factor ($\lambda = 6$) and using the proposed formula for calculating the period, the relations provided in the regulations are used to estimate the design base shear.
3. Using the first method with the assumption of the specified stability factor: In this method, using the proposed first method, assuming a stability

Table 1. The structural parameters of the three structures studied.

FRAME	V_u (KN)	M_t (KN.sec^2/cm)	V_d (KN)	G/h	ω_o/h (rad/sec)	τ
4S-3B	677.9	1.719	323.49	0.25	5.9179	1.18
10S-3BA	1702.63	6.803	820.00	0.22	2.6559	1.16
16S-2B	-1073.83	-	564.87	0.5625	1.7748	1.2

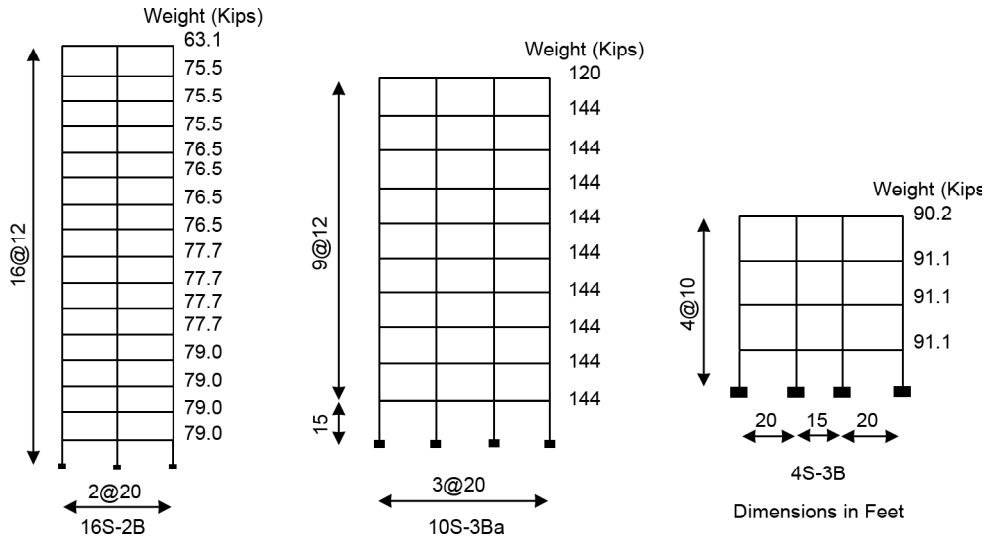

Figure 6. The dimensions and weight of the floors of the multi-story buildings used in this study; 4S-3B [20], 10S-3Ba [21], 16S-2B [22].

factor of 6 and 5, the overall failure behavior $(G/h=1.0)$ and the design displacement value (y_d), the expected bilinear curve for pushover behavior are calculated, based on which the amount of ultimate and critical displacement of the structure is calculated. The structure is finally redesigned to critical base shear, taking into account the nonlinear geometric effects. In this regard, after numerical studies, it can be concluded that the value of y_d is 1.5% for low-rise structures, 2% for mid-rise structures of 2%, and 2.5% for high-rise structures.

4. Using the first method with the assumption of the specified stability factor and the semi-rigid beam-column connection: The design base shear in this method is exactly the same as the value of method 3, and only the beam-column connection is assumed with 50% rigidity.
5. Using the first method with the assumption of the stability factor 5 and using simple framed beam connection and using the cable with a finite pre-stress coefficient: In this method, according to method 3, and assuming a stability factor of 5, the design base shear is computed, but in this case, all beam connections are modeled in pinned connection. However, limited prestressing cables are used to provide sufficient lateral load bearing capacity. The advantage of this method is firstly the simplicity of construction and installation of the structure, and secondly, in this method by changing the amount of prestressing force, there is better control over the performance of the structure.
6. Use of the second method: In this method, the value of yield displacement (y_y) is selected in ac cordance with the displacement of the Immediate Occupancy (IO) Level (based on FEMA 273 [19]) and the stability factor is chosen to the extent that the design displacement is at least equal to the proposed values in method 3. As a result, the critical base shear is considered as the design base shear and the structure is redesigned.
7. Using the second method with the semi-rigid beam-column connection: The base shear in this method is equal to the value calculated in method 6, and only in this method, the beam-column connection is assumed with 50% fixity.
8. Using the second method with the assumption of the stability factor 5 and using simple framed beam connection and using the cable with a finite pre-stress coefficient: The base cut of this method is also equal to the value calculated in method 6, but the structure, such as method 5, all beam connections are modeled in pinned connection. However, limited prestressing cables are used to provide sufficient lateral load bearing capacity.

Accordingly, the modeling results for the three structures are as follows. It should be noted that in this tables, T is the period of the structure, λ is the stability factor of the structure, λ_u is the stability factor after push, W is the weight of the structure, V is the seismic base shear, V_u is the ultimate base shear, δ_d is the displacement the same as S_{ac}.

It can be seen that the period of the 4-story frame from 1.13 (see Table 2), by using the proposed method, was increased to about 2.5 seconds without any stability problems. However, in this case, the stability of the structure is endangered after about 1.5% drift (method 4). It is also observed that using the cable with a finite pre-stressing (Method 5), the safety of the structure against the instability problem has been significantly improved.

Table 2. 4S-3B frame modeling results.

4S-3B	T (s)	λ	λ_u (1.5%)	λ_u (y_d%)	W (kN)	V (kN)	V_u (kN)	δ_d (%)
2800	1.13	21.95	18.07	12.97	1685.70	323.49	677.90	1.54
Tech. 1	1.28	21.18	10.95	3.76	1677.03	199.27	537.16	2.43
Tech. 2	1.46	15.36	6.28	4.63	1670.81	114.76	352.19	1.55
Tech. 3 (λ=6)	1.80	10.22	4.49	1.85	1663.40	56.45	273.62	2.71
Tech. 4 (λ=6)	2.58	5.04	4.40	1.60	1662.40	40.70	159.02	2.42
Tech. 3 (λ=5)	1.81	10.23	4.49	1.85	1662.68	53.11	273.62	2.71
Tech. 4 (λ=5)	2.51	5.34	5.20	4.14	1662.36	53.10	208.34	3.20
Tech. 5 (λ=5)	2.18	6.07	4.63	2.59	1710.48	54.58	352.25	3.45
Tech. 6 (λ=6)	1.78	10.46	4.80	1.05	1663.65	49.12	272.80	2.57

Table 3. 10S-3Ba frame modeling results.

10S-3Ba	T (s)	λ	λ_u (1.5%)	λ_u (y_d%)	W (kN)	V (kN)	V_u (kN)	δ_d (%)
2800	2.37	13.72	13.34	4.45	6671.47	820.00	1702.25	1.89
Tech. 1	4.62	3.89	3.18	1.00	6545.05	199.30	541.10	1.92
Tech. 2	3.63	6.77	6.67	1.92	6592.90	381.81	902.02	2.27
Tech. 3 (λ=6)	4.54	4.03	3.62	1.13	6549.32	225.99	548.17	1.79
Tech. 3 (λ=6, y_d = 2%)	4.01	5.36	4.65	0.29	6573.17	301.77	747.91	2.00
Tech. 3 (λ=5)	4.60	3.96	3.60	0.80	6547.62	209.14	542.90	1.87
Tech. 3 (λ=5, y_d = 2%)	4.21	4.93	4.31	0.95	6564.68	281.76	659.23	1.88
Tech. 6 (λ=9.5)	3.86	5.79	5.22	0.90	6580.54	323.90	774.92	2.00

Table 4. 16S-2B frame modeling results.

16S-2B	T (s)	λ	λ_u (1.5%)	λ_u (y_d%)	W (kN)	V (kN)	V_u (kN)	δ_d (%)
2800	3.57	11.74	12.74	6.67	5875.02	565.01	1073.63	1.95
Tech. 1	7.43	2.64	2.54	0.70	5688.87	95.39	263.38	2.40
Tech. 2	4.98	5.85	5.77	0.36	5776.58	278.58	606.94	1.96
Tech. 3 (λ=6)	5.54	4.65	4.57	0.21	5742.75	206.34	453.52	2.14
Tech. 3 (λ=6, y_d = 2%)	4.98	5.85	5.77	0.36	5776.58	276.87	606.94	1.96
Tech. 3 (λ=6, y_d = 2.5%)	4.41	7.51	7.43	0.32	5809.22	347.97	726.70	2.23
Tech. 3 (λ=5)	5.64	4.43	4.34	0.10	5736.46	189.05	452.59	2.31
Tech. 3 (λ=5, y_d = 2%)	5.16	5.58	5.52	0.76	5765.92	253.34	552.52	2.26
Tech. 3 (λ=5, y_d = 2.5%)	4.67	6.69	6.61	1.27	5791.86	318.07	643.95	2.35
Tech. 6 (λ=9.5)	4.29	7.90	7.83	1.27	5819.43	365.22	743.78	2.11

The period of the 10-story frame has also been increased to about 4.5 seconds. However, it is observed that the stability of the structure is endangered after 1.5% drift. Also, based on the above results, it is observed that the seismic base shear of the structure is reduced four times compared to the standard design method (Table 3).

In the case of the selected 16-story frame, it can be seen that the period has increased up to about 5.5 seconds while maintaining the stability of the structure up to 1.5% drift (Table 4).

It should be noted that the present study is limited to short to mid-rise moment frame structures and no comment is made on tall structures. Also, based on the hypotheses mentioned, it can be concluded that no structural irregularities are acceptable. It is also clear that in regular short-order structures the effects of higher modes are not very significant

5. Conclusion

In this paper, the stability of mass substructure in the mass isolation system (MIS) is investigated. MIS consists of two substructures and this research shows that for the optimal performance of this system, the period difference between the two substructures should be as large as possible. Increasing the period difference between the two substructures makes the dampers between them having good efficiency. To create a period difference between the two substructures and to reduce the seismic base shear, the soft substructure is designed for increasing the period and flexibility while maintaining its stability.

Therefore, the stability of the structure is investigated based on standards and articles, and then a relation for calculating the period of moment frame structures based on the structural stability factor is presented. Also, a relationship between the structural stability factor and the deflection amplification coefficient of deviation as well as the minimum safe stability factor of the structure with the assumption of safety factor 2 is presented.

Finally, with simple initial methods, the pushover bilinear curve of the structure is generated to achieve the maximum possible period. Based on the obtained curve, the seismic base shear is estimated and the structure is designed.

Using the proposed method in this paper, the period of the structure is increased up to two times, for example, the period of a 4-story structure is

increased from 1.13 to 2.5 seconds while maintaining stability. Of course, provided that the permissible displacement of the structure is limited, which is possible in the mass isolation system due to the presence of stiff substructure and dampers.

It should be noted that this is only a simplified preliminary method and the present study is limited to short to mid-rise moment frame structures, and due to the limited stability coefficient, any structural irregularities are not allowed and also the displacement of the structure should be limited. Also, since the proposed method is presented for regular short and mid-rise structures, the effect of higher modes is not very significant.

In the future, the proposed method can be improved by performing more detailed analyzes, including dynamic analysis or IDA, and also the hypotheses considered in this method can be examined more carefully.

References

1. Christenson, R.E., Spencer, B.F. J., Hori, N., and Seto, K. (2003) Coupled building control using acceleration feedback. *Computer-Aided Civil and Infrastructure Engineering*, **18**(1), 4-18, doi: http://dx.doi.org/10.1111/1467-8667.00295.

2. Yuji, K., Keizo, N., Masanori, I., Tamotsu, M., and Hirofumi, S. (2004) Development of connecting type actively controlled vibration control devices and application to high-rise triple buildings. *Engineering Review*, **37**(1).

3. Ziyaeifar, M. (2002) Mass Isolation, concept and techniques. *European Earthquake Engineering*, **2**(1), 43-55.

4. Ziyaeifar, M., Gidfar, S., and Nekooei, M. (2012) A model for Mass Isolation study in seismic design of structures. *Structural Control and Health Monitoring*, **19**(6), 627-645, doi:http://dx.doi.org/10.1002/stc.459.

5. Krawinkler, H., Zareian, F., Lignos, D.G., and Ibarra, L.F. (2009) Prediction of collapse of structures under earthquake excitations. *Proceedings of the 2nd International Conf. on Computational Methods in Structural Dynamics and Earth*quake Engineering (COMPDYN 2009).

6. Adam, C., Ibarra, L.F., and Krawinkler, H. (2004) *Evaluation of P-Delta Effects in Non-Deteriorating MDOF Structures from Equivalent SDOF Systems*.

7. ASCE (2010) *Commentary for Chapters 11-22 (Seismic)*. In Minimum Design Loads for Buildings and Other Structures.

8. Adam, C., and Jager, C. (2012) Seismic collapse capacity of basic inelastic structures vulnerable to the P?delta effect. *Earthquake Engineering & Structural Dynamics*, **41**(4), 775-793. doi:http://dx.doi.org/10.1002/eqe.1157.

9. Bernal, D., Nasseri, A., and Bulut, Y. (2006) *Instability Inducing Potential of Near Fault Ground Motions*.

10. Jager, C. and Adam, C. (2013) Influence of collapse definition and near-field effects on collapse capacity spectra. *Journal of Earthquake Engineering*, **17**(6), 859-878. doi:http://dx.doi.org/10.1080/13632469.2013.795842.

11. Miranda, E. and Akkar, S.D. (2003) Dynamic instability of simple structural systems. *Journal of Structural Engineering*, **129**(12), 1722-1726.

12. Bernal, D. (1992) Instability of buildings subjected to earthquakes. *Journal of Structural Engineering*, **118**(8), 2239-2260.

13. Bernal, D. (1998) Instability of buildings during seismic response. *Engineering Structures*, **20**(4-6), 496-502.

14. ASCE (2010) *Minimum Design Loads for Buildings and Other Structures (ASCE/SEI 7-10)*. Reston, Virginia: American Society of Civil Engineers.

15. Boujary, M. and Ziyaeifar, M. (2019) Design of mass isolated atructures with consideration of stability constraints. *Journal of Seismology & Earthquake Engineering (JSEE)*, **21**(3), 49-63.

16. Bernal, D. (1987) Amplification factors for inelastic dynamic P-Δ effects in earthquake analysis. *Earthquake Engineering and Structural Dynamics*, **15**, 635-651.

17. Castilla, E. and Lopez, O. (1980) Influence of

gravity loads in seismic response (in Spanish). *Bol. IMME*, **18**(67), 3-18.

18. ASCE (2016) *Minimum Design Loads for Buildings and Other Structures (ASCE/SEI 7-16)*. Reston, Virginia: American Society of Civil Engineers.

19. FEMA (1997) *NEHRP Guidelines for the Seismic Rehabilitation of Buildings (FEMA 273), "ATC-33 Project*". In. Washington, D.C.: Federal Emergency Management Agency.

20. Pique, J. (1976) *On the Use of Simple Models in Nonlinear Dynamic Analysis*. Retrieved from Massachusetts Inst. of Tech., Cambridge, Mass.

21. Anderson, J.C. and Bertero, V.V. (1987) Uncertainties in establishing design earthquakes. *Journal of Structural Engineering*, ASCE, **113**(8), 1709-1724.

22. Kordi, E.E. and Bernal, D. (1991) *Instability in Buildings Subjected to Earthquakes*. Retrieved from Northeastern Univ., Boston, Mass.